UNIVERSITY OF BIRMINGHAM
University of Birmingham Research at Birmingham

The amplitude-normalised area of a bipolar electrograms as a measure of local conduction delay in the heart

Winter, James; O'Shea, Christopher; Shattock, Michael J; Kirchhof, Paulus; Niederer, Steven; Pavlovic, Davor; Dhanjal, Tarvinder; Mendonca Costa, Caroline ; Anderson, Grace ; Mejborg, Veronique; Coronel, Ruben

License:
None: All rights reserved

Document Version
Peer reviewed version

Citation for published version (Harvard):
Winter, J, O'Shea, C, Shattock, MJ, Kirchhof, P, Niederer, S, Pavlovic, D, Dhanjal, T, Mendonca Costa, C, Anderson, G, Mejborg, V & Coronel, R 2020, 'The amplitude-normalised area of a bipolar electrograms as a measure of local conduction delay in the heart', *Frontiers in Physiology*.

Link to publication on Research at Birmingham portal

General rights
Unless a licence is specified above, all rights (including copyright and moral rights) in this document are retained by the authors and/or the copyright holders. The express permission of the copyright holder must be obtained for any use of this material other than for purposes permitted by law.

• Users may freely distribute the URL that is used to identify this publication.
• Users may download and/or print one copy of the publication from the University of Birmingham research portal for the purpose of private study or non-commercial research.
• User may use extracts from the document in line with the concept of ‘fair dealing’ under the Copyright, Designs and Patents Act 1988 (?)
• Users may not further distribute the material nor use it for the purposes of commercial gain.

Where a licence is displayed above, please note the terms and conditions of the licence govern your use of this document.

When citing, please reference the published version.

Take down policy
While the University of Birmingham exercises care and attention in making items available there are rare occasions when an item has been uploaded in error or has been deemed to be commercially or otherwise sensitive.

If you believe that this is the case for this document, please contact UBIRA@lists.bham.ac.uk providing details and we will remove access to the work immediately and investigate.

Download date: 14. Jun. 2020

The amplitude-normalised area of a bipolar electrograms as a measure of local conduction delay in the heart

Caroline Mendonca Costa[1], Grace Anderson[2], Veronique Meijborg[3], Christopher O'Shea[4], Michael J. Shattock[2], Paulus Kirchhof[4, 5, 6], Ruben Coronel[3, 7], Steven A. Niederer[1], Davor Pavlovic[4], Tarvinder Dhanjal[8], James Winter[4*]

[1]School of Biomedical Engineering and Imaging Sciences, King's College London, United Kingdom, [2]School of Cardiovascular Medicine & Sciences, Faculty of Life Sciences & Medicine, King's College London, United Kingdom, [3]Amsterdam University Medical Center (UMC), Netherlands, [4]Institute of Cardiovascular Sciences, College of Medical and Dental Sciences, University of Birmingham, United Kingdom, [5]Department of Cardiology, UHB NHS Foundation Trust, United Kingdom, [6]Department of Cardiology, SWBH NHS Trust, United Kingdom, [7]Institut de rythmologie et modélisation cardiaque (IHU-Liryc), France, [8]University Hospitals Coventry and Warwickshire NHS Trust, United Kingdom

In review

Submitted to Journal:
Frontiers in Physiology

Specialty Section:
Cardiac Electrophysiology

Article type:
Original Research Article

Manuscript ID:
518523

Received on:
08 Dec 2019

Revised on:
30 Mar 2020

Frontiers website link:
www.frontiersin.org

Conflict of interest statement

The authors declare that the research was conducted in the absence of any commercial or financial relationships that could be construed as a potential conflict of interest

Author contribution statement

JW and DP developed the concept and designed the experiments. GA, VM, CO, DP & JW conducted the experimental studies and analysed the results. CMC and SM conducted the computational simulations. PK, RC and TD provided expert advice and direction. All authors reviewed and contributed to the final manuscript.

Keywords

Electrophysiology, Bipolar electrogram, Conduction delay, Substrate mapping, cardiac arrhythmia, Cardiac mapping

In review

Abstract

Word count: 324

Background

Re-entrant ventricular tachycardia may be non-inducible or haemodynamically compromising, requiring assessment of the electrophysiological properties of the myocardium during sinus rhythm (i.e. substrate mapping). Areas of heart tissue with slow conduction can act as a critical isthmus for re-entrant electrical excitation and are a potential target for ablation therapy.

Aim

To develop and validate a novel metric of local conduction delay in the heart, the amplitude-normalised electrogram area (norm_EA).

Methods

A computational model of a propagating mouse action potential was used to establish the impact of altering sodium channel conductance, intracellular conductivity, fibrosis density, and electrode size/orientation on bipolar electrogram morphology. Findings were then validated in experimental studies in mouse and guinea pig hearts instrumented for the recording of bipolar electrograms from a multipolar linear mapping catheter. norm_EA was calculated by integrating the absolute area of a bipolar electrogram divided by the electrogram amplitude. Electrogram metrics were correlated with the local conduction delay during sodium channel block, gap junction inhibition, and acute ischaemia.

Results

In computational simulations, reducing sodium channel conductance and intracellular conductivity resulted in a decrease in signal amplitude and increase in norm_EA (reflecting a broadening of electrogram morphology). For larger electrodes (3mm diameter/ 7.1mm2 area), the change in norm_EA was essentially linear with the change in local conduction delay. Experimental studies supported this finding, showing that the magnitude of change in norm_EA induced by flecainide (1-[illegible] M), carbenoxolone (10-50[illegible]M), and low-flow ischaemia (10% of initial flow rate) was linearly correlated with the local conduction delay in each condition (r2=0.92). Qualitatively similar effects were observed in guinea pig hearts perfused with flecainide. Increasing fibrosis density also resulted in a decrease in signal amplitude and increase in norm_EA. However, this remains to be validated using experimental/clinical data of chronic infarct.

Conclusion

norm_EA is a quantitative measure of local conduction delay between the electrode pair that generates a bipolar electrogram, which may have utility in electrophysiological substrate mapping of non-inducible or haemodynamically compromising tachyarrhythmia.

Contribution to the field

Electrophysiological mapping using intracardiac electrograms is used in the treatment of abnormal heart rhythms (cardiac arrhythmias). Re-entrant ventricular tachycardia is often non-inducible or haemodynamically compromising, necessitating the assessment of the electrophysiological properties of the myocardium during sinus rhythm (i.e. substrate mapping). Information collected in substrate mapping is used to guide catheter ablation therapy. The present study describes a new analytical approach to substrate mapping, applying a combined computation and experimental approach to develop and validate a novel metric of local conduction delay in the heart, which may have application in substrate mapping procedures (i.e. to identify regions of abnormally slow conduction, that may act as an isthmus for re-entrant ventricular tachycardia).

Funding statement

JW (FS/16/35/31952) is supported by the British Heart Foundation. DP and CO are supported by the (Sci-Phy-4-Health Centre for Doctoral Training L016346) EPSRC, (109604/Z/15/Z) Wellcome Trust and (PG/17/55/33087, FS/16/35/31952, FS/19/16/34169, FS/19/12/34204) British Heart Foundation. RC, VM are supported by a Transatlantic Network of Excellence grant from the Leducq Foundation (16CVD02, RHYTHM). GA and MJS are supported by the British Heart Foundation. CMC is supported by the British Heart Foundation (PG/15/91/31812). This work was further supported by European Union (grant agreement No 633196 [CATCH ME]), European Union BigData@Heart (grant agreement EU IMI 116074), British Heart Foundation (FS/13/43/30324; PG/17/30/32961, and AA/18/2/34218), and Leducq Foundation (genomic topology of AF to PK).

Ethics statements

Studies involving animal subjects

Generated Statement: The animal study was reviewed and approved by Birmingham University and King's College London Animal Welfare and Ethics Review Committees.

Studies involving human subjects

Generated Statement: No human studies are presented in this manuscript.

Inclusion of identifiable human data

Generated Statement: No potentially identifiable human images or data is presented in this study.

Data availability statement

Generated Statement: The datasets generated for this study are available on request to the corresponding author.

In review

The amplitude-normalised area of a bipolar electrograms as a measure of local conduction delay in the heart

Caroline Mendonca Costa[1], Grace Anderson[2], Veronique Meijborg[3], Christopher O'Shea[4], Michael J. Shattock[2], Paulus Kirchhof[4,4a,4b], Ruben Coronel[3,6], Steven Niederer[1], Davor Pavlovic[4], Tarvinder Dhanjal[5], James Winter[4*]

[1]Department of Biomedical Engineering, King's College London, SE1 7EH

[2]School of Cardiovascular Medicine & Sciences, King's College London, SE1 7EH

[3]Department of Experimental Cardiology, Academic Medical Center, Amsterdam, The Netherlands

[4]Institute of Cardiovascular Science, University of Birmingham, B15 2TT

4a Department of Cardiology, UHB NHS Foundation Trust

4b Department of Cardiology, SWBH NHS Trust

[5]University Hospitals Coventry and Warwickshire, Coventry, CV2 2DX

[6] Heart Arrhythmia and Modelling Institute, LIRYC, Pessac, France

*Corresponding author

Dr James Winter

Institute of Cardiovascular Sciences

University of Birmingham

B15 2TT

J.Winter.1@bham.ac.uk

Word count: 3825 (including abstract and main body).

In review

Abstract (296 words)

Background

Re-entrant ventricular tachycardia may be non-inducible or haemodynamically compromising, requiring assessment of the electrophysiological properties of the myocardium during sinus rhythm (i.e. substrate mapping). Areas of heart tissue with slow conduction can act as a critical isthmus for re-entrant electrical excitation and are a potential target for ablation therapy.

Aim

To develop and validate a novel metric of local conduction delay in the heart, the amplitude-normalised electrogram area (norm_EA).

Methods

A computational model of a propagating mouse action potential was used to establish the impact of altering sodium channel conductance, intracellular conductivity, fibrosis density, and electrode size/orientation on bipolar electrogram morphology. Findings were then validated in experimental studies in mouse and guinea pig hearts instrumented for the recording of bipolar electrograms from a multipolar linear mapping catheter. norm_EA was calculated by integrating the absolute area of a bipolar electrogram divided by the electrogram amplitude. Electrogram metrics were correlated with the local conduction delay during sodium channel block, gap junction inhibition, and acute ischaemia.

Results

In computational simulations, reducing sodium channel conductance and intracellular conductivity resulted in a decrease in signal amplitude and increase in norm_EA (reflecting a broadening of electrogram morphology). For larger electrodes (3mm diameter/ 7.1mm^2 area), the change in norm_EA was essentially linear with the change in local conduction delay. Experimental studies supported this finding, showing that the magnitude of change in norm_EA induced by flecainide (1-3μM), carbenoxolone (10-50μM), and low-flow ischaemia (10% of initial flow rate) was linearly correlated with the local conduction delay in each condition (r^2=0.92). Qualitatively similar effects were observed in guinea pig hearts perfused with flecainide. Increasing fibrosis density also resulted in a decrease in signal amplitude and increase in norm_EA. However, this remains to be validated using experimental/clinical data of chronic infarct.

Conclusion

In review

norm_EA is a quantitative measure of local conduction delay between the electrode pair that generates a bipolar electrogram, which may have utility in electrophysiological substrate mapping of non-inducible or haemodynamically compromising tachyarrhythmia.

In review

1. Introduction

Substrate mapping of the ventricular myocardium is an electrophysiological mapping modality that is commonly applied when the culprit arrhythmia cannot be induced or is hemodynamically compromising.(1, 2) It is typically performed during electrical pacing or in sinus rhythm.(1) Substrate mapping metrics such as bipolar electrogram voltage (amplitude), fractionation, and late/split/double potentials are used to define regions of tissue that are deemed critical to the initiation and maintenance of re-entrant tachycardia (i.e. the isthmus of the circuit) and are therefore a target for radiofrequency ablation therapy.(3) The conduction of electrical impulses in such regions is typically slow when compared to the normal myocardium, usually as a result of injury and tissue remodelling. For example, in ventricular scar formed after myocardial infarction, conduction is typically delayed by the tortuous pattern of activation through surviving myocardial fibres found within the scar tissue.(4)

A means to assess regions of tissue where there is abnormally slow conduction during substrate mapping could allow better targeting of ablation therapy. One already established metric is the duration of the activation components of the bipolar electrogram. Theoretically, an increase in the conduction time (greater conduction delay) between the two recording electrodes results in a broader electrogram morphology.(5) Indeed, it is already known that prolonged bipolar electrogram duration is a characteristic of heart disease and of electrograms recorded from and around ventricular scar tissue.(6-10) However, electrogram duration is not a widely used metric in substrate mapping procedures. This may reflect the ambiguity in defining the start and end of the electrogram complexes, which is particularly relevant for low-amplitude-signals, as well as the fact that automated measurements of electrogram duration are susceptible to errors caused by signal artefacts. To address these limitations, we sought to develop an alternative, algorithmically calculable and quantitative metric of conduction delay with potential application in electrophysiological substrate mapping procedures.

The total area of the activation components of a bipolar electrogram is a function of electrogram amplitude, electrogram duration, the number of peaks and troughs within the signal and the diameter of the recording electrode. Delayed or slowed electrical conduction in the tissues underlying the recording electrodes would be expected to both reduce signal amplitude and prolong electrogram duration, acting to decrease and increase the area of the electrogram, respectively. We hypothesised that the absolute electrogram area (EA) normalised to the signal amplitude, herein referred to as normalised EA (norm_EA), could be used as a quantitative

In review

index of local conduction delay. The present study uses a combination of computational modelling and experimental studies in mammalian hearts to test this hypothesis.

In review

2. Methods

2.1 Computational modelling

A 3D mesh of hexahedral elements was created representing a sheet of myocardium covered by a thin layer of bath (see Figure 1). Myocardium and bath dimensions are each 10x10x0.01mm. Mesh elements have a mean resolution of 0.01mm. Cardiac electrophysiology was simulated using the cardiac bidomain model of action potential propagation coupled with the Bondakenko(11) model of the action potential of mouse ventricular myocytes. Simulations were run using the Cardiac Arrhythmia Research Package (CARP)(12). Tissue conductivities were tuned(13) to yield a conduction velocity of ~0.75 m/s, comparable with experimentally measured values in mouse heart.(14) Isotropic intracellular and extracellular conductivities of 0.7 S/m and 1.03 S/m, respectively, were assigned to the bidomain model.

Bipolar electrograms were recorded from the centre of the tissue with (unless stated otherwise) 0.1mm electrode diameter and electrode spacing of 1mm, see Figure 1. Pacing stimuli were delivered to the tissue edge to generate a wavefront that propagated parallel to the orientation of the recording electrodes. The effect of conduction slowing on electrogram morphology was investigated by decreasing the sodium channel conductance (gNa) and the intracellular conductivity (σ_i), separately, in a stepwise manner from 100 to 10% of the initial model parameters

It is known that electrode diameter affects electrogram morphology due to spatial averaging.(15) We have investigated the impact of electrogram diameter in our simulations by averaging the signal of mesh nodes within a circle (as depicted in Figure 1– green circles) with diameter varying from 0.1 to 3.0 mm in steps of 0.1 mm. Spacing between the electrodes was preserved at 1mm (edge-to-edge).

Fibrosis was included in circular region (radius = 2mm) in the middle of the slab. Different fibrosis densities were modelled, namely 20, 40, 60, 80, and 100%. This was achieved by randomly selecting the desired percentage of finite elements within the fibrosis region and removing these from the intracellular grid but not the extracellular grid, thus allowing, extracellular signals (electrograms) to be computed. This effectively models fibrosis as non-conducting tissue, as done previously.(16)

Activation times were measured as the time at which the local action potential reached maximum upstroke velocity (dV/dt). Action potentials were averaged according to electrode size, as done for electrograms.

In review

2.2 Experimental studies

2.2.1 Animal welfare/ethics

All procedures were undertaken in accordance with ethical guidelines set out by the UK Animals (Scientific Procedures) Act 1986 and Directive 2010/63/EU of the European Parliament on the protection of animals used for scientific purposes. Studies conformed to the Guide for the Care and Use of Laboratory Animals published by the U.S. National Institutes of Health under assurance number A5634-01. The procedures had been approved by the University of Birmingham and King's College London Animal Welfare and Ethical Review Boards.

2.2.2 Isolated heart studies

Mouse (C57/BL6, 25-30g, Charles River, UK) hearts were isolated under isoflurane-induced anaesthesia (4% in 100% O_2) with concomitant intraperitoneal injection of heparin (100units injected 5-minutes before heart isolation). Hearts were Langendorff-perfused via the aorta at a perfusion pressure of 70-80mmHg with an oxygenated (95% O_2 5% CO_2) crystalloid buffer, containing (in mM); NaCl 114, KCl 4, CaCl 1.4, $NaHCO_3$ 24, NaH_2PO_4 1.1, glucose 11.0 and sodium pyruvate 1.0 (pH 7.4, 37^{o}C).

Guinea pig hearts (Dunkin Hartley, Marshall BioResources, 450-550g) were isolated under sodium pentobabitone (160mg/kg, i.p.) induced anaesthesia with concomitant injection of heparin (150units). Hearts were Langendorff perfused via the aorta at a perfusion pressure of 60-70mmHg with an oxygenated (ibidem) crystalloid buffer, containing (in mM); NaCl 114, KCl 4, CaCl 1.8, $NaHCO_3$ 24, NaH_2PO_4 1.1, glucose 11.0 and sodium pyruvate 1.0 (pH 7.4, 37^{o}C).

2.2.3 Protocols

An 8 pole electrophysiological mapping catheter was inserted into the left ventricular lumen via a small incision in the left atrium. Between four and five unipolar electrograms (poles 4-8) were recorded from endocardial surface of the left ventricular free wall. Reference and ground electrodes were placed in the perfusion chamber (~3cm from the heart). The catheter diameter was 1mm and electrode height was 1mm, giving a total electrode surface area of 3.14mm^2. Three to four bipolar electrograms were calculated from adjacent poles (1mm spacing) according to the method of Blanchard *et al.*(17) All data were digitised at 4kHz with 0.2Hz high-pass and 1000Hz low-pass filters (OctalBioamp and PowerLab 16s, ADInstruments, Australia).

In review

Mouse hearts were paced at 3x the diastolic threshold via the two distal poles on the mapping catheter (endocardial pacing, 420 bpm, 1ms pulse duration). Interventions to alter ventricular conduction were (i) 3-minutes of low-flow global ischaemia (25% of initial flow rate), (ii) increasing concentrations of the sodium channel blocker flecainide (1-4μmol/L), and (iii) increasing concentrations of the gap junction inhibitor carbenoxolone (10-50μmol/L).

Guinea pig hearts were allowed to beat at their intrinsic (sinus) rate and after a baseline stability period, were perfused with flecainide (4μmol/L).

2.3 Calculation of normalised electrogram area (norm_EA)

EA was derived by measuring the integrated area of the electrogram above and below a baseline noise threshold of ±0.05mV over a fixed time window of 300ms. A diagrammatic representation of the methodology is presented in Figure 2. The red area indicates the integrated area of the bipolar electrogram. The maximum value of the absolute cumulative area shown in Figure 1b equates to the total EA. norm_EA was calculated by dividing the total EA by the electrogram amplitude (maximum – minimum). Conduction delay was calculated from the difference in the activation time of the unipolar electrogram between each adjacent pair of electrodes, where activation time was taken as the time of minimum dV/dt of the unipolar signals.

In review

2.4 Statistical analysis

Statistical comparisons were made by 1-way repeated measures ANOVA with Bonferroni post-hoc tests. Statistical significance was taken as $p<0.05$. Average data are presented as mean±SEM with replicate values shown in grey.

3. Results

3.1 Computational modelling

The effects of conduction slowing via reduced gNa and σ_i were investigated using a computational model of a propagating mouse ventricular action potential (as described in the Methods). Results for the simulations are presented in Figure 3-5. Traces in Figure 3a show simulated electrograms for varying levels of gNa and σ_i (as a % of initial model values). Decreasing either gNA or σ_i resulted in a reduction in bipolar electrogram amplitude and a broadening of electrogram morphology. The coloured regions in Figure 3a indicate the electrogram area. Quantitative analysis of the change in signal amplitude and EA are shown in Figure 3b-d. A reduction in either model parameter led to a decrease in electrogram amplitude (Figure 3b), whereas altering gNA and σ_i had divergent effects on the absolute EA (Figure 3c). The traces in Figure 3a show that whilst both parameters altered electrogram morphology, the effects on electrogram amplitude and duration were intervention-dependent. Altering gNA exerted a greater effect on electrogram duration vs. amplitude and altering σ_i had a greater effect on electrogram amplitude vs. duration. The change in absolute EA (Figure 3c) reflects the balance of these effects. Figure 3d shows absolute EA values normalised to electrogram amplitude, thus representing the amplitude-independent EA, norm_EA. norm_EA increased in response to reduced gNa and σ_i, but to a greater degree in the former, consistent with more pronounced broadening of electrogram morphology for a given % change in gNa vs. σ_i.

Data presented in Figure 4a-c show the relationship between norm_EA and conduction delay between the two recording electrodes. Results are presented for electrode diameters of 0.1, 1.0 and 3.0mm (electrode spacing was kept constant at 1mm from edge-to-edge (see Supplementary Figure 1)). Figure 4a presents data for the smallest recording electrode diameter (0.1mm) and shows that the reduction of either gNA or σ_i caused an increase in the norm_EA as greater conduction delays are induced (slower conduction velocity). However, the absolute relationship between the variables differed for each intervention (Figure 4a). Corresponding norm_EA and conduction delay curves for simulations using larger electrode diameters are shown in Figures 4b and 4c. Notably, increasing the electrode diameter, which results in larger spatial signal averaging across the tissue, led to an increase in baseline norm_EA and the convergence of the gNa and σ_i curves (Figures 4b&c). Thus, at clinically relevant electrode sizes (1.0-3.0mm), the norm_EA of a bipolar electrogram is a direct function of the conduction delay between the two recording electrodes. Notably, this is not the case for bipolar electrogram

In review

amplitude, as we found that increasing the electrode diameter led to greater divergence of the amplitude-conduction delay curves, as shown in Figure 4d-f.

Figure 5 presents data on the effects of altering the orientation of the recording electrodes relative to the direction wavefront propagation on electrogram morphology within the previously discussed model. The presented angles are relative to the initial orientation of the electrodes, as illustrated in Figure 5a. The effects of altering the electrode orientation from 0 to 90^{O} on electrogram amplitude and norm_EA at varying levels of σ_i are shown in Figure 5a&b, respectively. As the electrode-wavefront angle was increased, both signal amplitude and norm_EA reduced (with no signal recorded when the electrodes were exactly perpendicular to the direction of wavefront propagation – data not shown). Similar results were observed for different levels of $\sigma_{i,}$ though the absolute magnitude and change in each variable differed for each simulation. The data shown in Figure 5d&e show the same data plotted against the local conduction delay between the electrode pair. Notably, whereas the relationship between signal amplitude and local conduction delay was non-linear and dependent on the level of $\sigma_{i,}$, the relationship between norm_EA and conduction delay was found to be linear. Thus, norm_EA was again found to be proportional to the local conduction delay between the electrode pair that make up the bipolar electrogram, irrespective of whether this delay was due to slowed conduction (i.e. via reduced σ_i) or the orientation of the electrodes relative to the direction of the propagating activation wavefront.

Figure 6 presents data on the impact of simulated regional fibrosis on the pattern of electrical activation and electrogram morphology. Activation (derived from a 10x10 grid of unipolar signals), and calculated bipolar voltage and norm_EA maps are shown for varying degrees of fibrosis (20-100%) within a circular region of tissue. Increasing levels of fibrosis were associated with slowing of conduction (as evidenced by the crowding of the isochronal lines), a reduction in bipolar electrogram amplitude and a decrease in norm_EA. Notably, regional electrograms were observed even at 100% fibrosis, as finite elements labelled as fibrotic are only removed from the intracellular grid. Quantitative analysis of electrograms recorded within the fibrotic core region showed a linear reduction in amplitude and increase in norm_EA as a function of increasing conduction delay, as presented in Figure 7. Visual inspection shows greater spatial association between fibrotic regions and increased norm_EA than amplitude, although these associations were not quantified in this study.

In review

3.2 Experimental studies

3.2.1 Studies in isolated mouse hearts

Data presented in Figure 8 show the effects of the sodium channel blocker flecainide and gap junction inhibitor carbenoxolone on the morphology of bipolar electrograms recorded from the endocardial surface of the mouse left ventricle. This replicates experimentally the effects of reduced gNa and σ_i in the computational model. Data showing concentration-dependent changes in bipolar amplitude, absolute EA and norm_EA are presented in panels a-c for flecainide and panels d-e for carbenoxolone. At 30μmol/L, carbenoxolone caused a substantive decrease in electrogram amplitude. A similar, but smaller, effect was observed with flecainide. One outlier result prevented this effect being statistically significant. Consistent with the computational simulations, the concentration-dependent change in absolute EA was different for each treatment, increasing in response to flecainide and decreasing with carbenoxolone. Meanwhile, norm_EA increased in a concentration-dependent manner for both treatments.

Figure 9 presents data on the impact of low-flow global ischaemia and reperfusion on electrogram morphology in the mouse heart; a pathophysiological cause of conduction slowing. Figure 9a shows the changes in electrogram morphology associated with a 2-minute period of low-flow ischaemia at 25% of the initial flow rate. During low-flow perfusion, a reduction in amplitude and broadening of the bipolar electrogram was observed, which rapidly recovered to initial values on tissue reperfusion. Summary data for changes in signal amplitude, absolute EA and norm_EA are shown in Figure 9b-d. The results are consistent with the effects of reduced sodium channel availability. Ischaemia was associated with a reduction in signal amplitude, no change in absolute EA and an increase in norm_EA. All values normalised on tissue reperfusion.

Data presented in Figure 10 shows that norm_EA and signal amplitude are stable in experimental recordings made without the study interventions, indicating that the changes observed for flecainide, carbenoxolone and ischaemia were due to their direct biological action.

Figure 8g shows the relationship between norm_EA and local conduction delay; as measured from the mean difference in activation time between adjacent unipolar electrogram recordings. A strong linear correlation was observed (r^2=0.92, p<0.0001), with data from low-flow ischaemia, flecainide and carbenoxolone protocols falling on the same linear relationship. In contrast, the relation between bipolar electrogram amplitude and local conduction delay diverges from a linear relationship (panel h, r^2=0.70, p<0.0001).

In review

3.2.2 Studies in isolated guinea pig hearts

We next investigated the impact of sodium channel block on bipolar norm_EA in isolated perfused guinea pig hearts, which have similar action potential morphology and ion channel expression as that of the human heart. Guinea pig hearts, beating at their intrinsic rate, were perfused with a standard crystalloid buffer, before switching to a buffer solution containing 4μmol/L of flecainide. A marked reduction in amplitude and increase in norm_EA was observed, which is shown in in Figure 11a&b, and is consistent with those observed in perfused mouse hearts (Figure 68).

In review

4. Discussion

Using computational modelling and experimental studies performed in isolated mammalian hearts, the present study presents data in support of a novel metric of local conduction delay in the heart - that of the norm_EA of a bipolar elecrogram. In mouse hearts, we found that the change in norm_EA was directly proportional to the change in local conduction delay between closely spaced (bipolar) recording electrodes and that this relationship was independent of the mechanism by which a change in conductuin delay was achieved (i.e. sodium channel block, gap junction inhibition and ischaemia). Meanwhile, bipolar electrogram amplitude, a commonly used metric in substrate mapping procedures, was found to be differentially impacted by the effects of sodium channel block and gap junction inhibition. Whilst altering electrode orientation had a marked impact on electrogram morphology in our simulation studies, our results indicate that the change in norm_EA remains proportional to the degree of conduction delay between the recording electrodes, which is of course influenced by tissue conduction velocity, but also the spacing between the electrodes and their position relative to the activation wavefront. This finding remained true for a range of model parameters, which was notably not the case for bipolar electrogram amplitude. On the basis of these results, we conclude that the norm_EA of a bipolar electrogram is a quantitative index of temporal difference in activation time of the tissue near to the recording electrodes, at least in the mouse heart. We also recorded qualitatively similar changes in electrogram morphology in guinea pig hearts perfused with flecainide, as those observed in the mouse heart, suggesting our findings may be more broadly applicable to other species.

Theoretically, an increase in conduction delay in the heart will result in a broadening of the QRS-morphology of an electrogram recorded from two closely spaced poles (i.e. a bipolar electrogram). Local conduction delay could therefore be quantified by measuring the duration of the corresponding electrograms. However, whilst electrogram duration is relatively easy to measure for electrograms recorded from healthy tissue, it becomes more difficult to define accurately for the low-amplitude, multiphasic signals often recorded in and around fibrotic and scarred tissue. A major limitation is that electrogram duration depends on the correct placement of only two points relative to the activation front, and, therefore it is particularly sensitive to errors caused by signal artefacts and noise, resulting in incorrect labelling of the start and end of the electrogram complexes. Such ambiguity is avoided (or at least limited) in the norm_EA metric, where integration of the total electrogram area is less sensitive to both signal artefacts and noise. Notably, the norm_EA metric is also easy to calculate and computationally

In review

inexpensive, and so could be easily integrated into existing electroanatomical mapping platforms/software. However, it is recognised that the total area of the electrogram is not simply a function of amplitude and duration, but of the overall morphology of the electrogram, including the number, shape and relative size of the peaks and troughs within the signal. Thus, norm_EA is not a direct surrogate for electrogram duration, but a complex measure that is influenced by multiple factors. In the present study, we have generated evidence showing that the norm_EA is directly proportional to the conduction delay between the recording electrodes of a bipolar electrogram. Notably, similar relationships have not been established for other substrate mapping metrics.

In simulation studies, we found that delays in activation caused by fibrosis (modelled as different densities (20-100%) of non-conducting tissue) led to a linear decrease and increase in signal amplitude and norm_EA, respectively, when considering electrograms in the centre of the fibrotic region. This would imply that both bipolar electrogram amplitude and norm_EA are accurate measures of local conduction delays due to fibrosis and the resulting tortuous pattern of activation through the remaining tissue. However, norm_EA appears to better correlate spatially with regions fibrosis than amplitude (Figure 6), although we did not quantify this relationship. Determining this spatial correlation would require more complex computational models, which account for realist infarct scar morphology and wall thickness, defining voltage and norm_AE thresholds, and validating these against clinical data of chronic infarct patients.(18) Such detailed investigation is out of the scope of this proof-of-concept study.

Whilst the present study does not address the efficacy of the norm_EA metric in substrate mapping procedures, clinical testing is a clear goal of future research. Instead, the present work provides good evidence in support of the norm_EA metric in the assessment of local conduction delay in the heart, which feasibly has utility for the mapping of pro-arrhythmogenic substrate in non-inducible and haemodynamically unstable arrhythmia, such as scar-related ventricular tachycardia.

4.2 Conclusion

Using a combined computation and experimental approach, this study provides evidence that norm_EA of a bipolar electrogram is a quantitative index of local conduction delay in the tissue close to the recording electrodes. This novel metric may have utility in electrophysiological

In review

substrate mapping procedures, but further validation in a model of chronic myocardial infarction is required.

Sources of funding

JW (FS/16/35/31952) is supported by the British Heart Foundation. DP and CO are supported by the (Sci-Phy-4-Health Centre for Doctoral Training L016346) EPSRC, (109604/Z/15/Z) Wellcome Trust and (PG/17/55/33087, FS/16/35/31952, FS/19/16/34169, FS/19/12/34204) British Heart Foundation. RC, VM are supported by a Transatlantic Network of Excellence grant from the Leducq Foundation (16CVD02, RHYTHM). GA and MJS are supported by the British Heart Foundation. CMC is supported by the British Heart Foundation (PG/15/91/31812). This work was further supported by European Union (grant agreement No 633196 [CATCH ME]), European Union BigData@Heart (grant agreement EU IMI 116074), British Heart Foundation (FS/13/43/30324; PG/17/30/32961, and AA/18/2/34218), and Leducq Foundation (genomic topology of AF to PK).

Financial disclosures

PK receives research support for basic, translational, and clinical research projects from European Union, British Heart Foundation, Leducq Foundation, Medical Research Council (UK), and German Centre for Cardiovascular Research, from several drug and device companies active in atrial fibrillation, and has received honoraria from several such companies in the past. PK is listed as inventor on two patents held by University of Birmingham (Atrial Fibrillation Therapy WO 2015140571, Markers for Atrial Fibrillation WO 2016012783).

In review

5. References

1. Pedersen CT, Kay GN, Kalman J, Borggrefe M, Della-Bella P, Dickfeld T, et al. EHRA/HRS/APHRS expert consensus on ventricular arrhythmias. *Europace* (2014) 16(9):1257-83. doi: 10.1093/europace/euu194.

2. Priori SG, Blomstrom-Lundqvist C, Mazzanti A, Blom N, Borggrefe M, Camm J, et al. 2015 ESC Guidelines for the management of patients with ventricular arrhythmias and the prevention of sudden cardiac death: The Task Force for the Management of Patients with Ventricular Arrhythmias and the Prevention of Sudden Cardiac Death of the European Society of Cardiology (ESC)Endorsed by: Association for European Paediatric and Congenital Cardiology (AEPC). *Europace* (2015) 17(11):1601-87. doi: 10.1093/europace/euv319.

3. Josephson ME, Anter E. Substrate Mapping for Ventricular Tachycardia. Assumptions and Misconceptions. *J Am Coll Cardiol* (2015) 1(5):341-52. doi: 10.1016/j.jacep.2015.09.001.

4. de Baker JMT, Coronel R, Tasseron S, Wilde AAM, Opthof T, Janse MJ, et al. Ventricular tachyrdia in the infarcted, Langendorff-perfused human heart: Role of the arrangement of surviving cardiac fibers. *J Am Coll Cardiol* (1990) 15(7):1594-607. doi: 10.1016/0735-1097(90)92832-m.

5. Venkatachalam KL, Herbrandson JE, Asirvatham SJ. Signals and Signal Processing for the Electrophysiologist. *Circ Arrhythm Electrophysiol* (2011) 4(6):974-81. doi: 10.1161/CIRCEP.111.964973.

6. Cassidy DM, Vassallo JA, Marchlinski FE, Buxton AE, Untereker WJ, Josephson ME. Endocardial mapping in humans in sinus rhythm with normal left ventricles: activation patterns and characteristics of electrograms. *Circ* (1984) 70(1):37-42. doi: 10.1161/01.CIR.70.1.37.

7. Cassidy DM, Vassallo JA, Miller JM, Poll DS, Buxton AE, Marchlinski FE, et al. Endocardial catheter mapping in patients in sinus rhythm: relationship to underlying heart disease and ventricular arrhythmias. *Circ* (1986) 73(4):645-52. doi: 10.1161/01.CIR.73.4.645.

8. Cassidy DM, Vassallo JA, Buxton AE, Doherty JU, Marchlinski FE, Josephson ME. The value of catheter mapping during sinus rhythm to localize site of origin of ventricular tachycardia. *Circ* (1984) 69(6):1103-10. doi: 10.1161/01.cir.69.6.1103.

9. Untereker WJ, Spielman SR, Waxman HL, Horowitz LN, Josephson ME. Ventricular activation in normal sinus rhythm: abnormalities with recurrent sustained tachycardia and a history of myocardial infarction. *Am J Cardiol* (1985) 55(8):974-9. doi: 10.1016/0002-9149(85)90729-5.

10. Vassallo JA, Cassidy DM, Marchlinski FE, Miller JM, Buxton AE, Josephson ME. Abnormalities of endocardial activation pattern in patients with previous healed myocardial infarction and ventricular tachycardia. *Am J Cardiol* (1986) 58(6):479-84. doi: 10.1016/0002-9149(86)90019-6.

11. Bondarenko VE, Szigeti GP, Bett GCL, Kim S-J, Rasmusson RL. Computer model of action potential of mouse ventricular myocytes. Am J Physiol Heart Circ Physiol (2004) 287(3):H1378-H403. doi: 10.1152/ajpheart.00185.2003.

In review

12. Vigmond EJ, Hughes M, Plank G, Leon LJ. Computational tools for modeling electrical activity in cardiac tissue. *Journal of Electrocardiology* (2003) 36:69-74. doi: /10.1016/j.jelectrocard.2003.09.017.

13. Costa CM, Hoetzl E, Rocha BM, Prassl AJ, Plank G. Automatic Parameterization Strategy for Cardiac Electrophysiology Simulations. *Comp Cardiol* (2013) 40:373-6.

14. Boukens BJ, Sylva M, de Gier-de Vries C, Remme CA, Bezzina CR, Christoffels VM, et al. Reduced sodium channel function unmasks residual embryonic slow conduction in the adult right ventricular outflow tract. *Circ Res* (2013) 113(2):137-41. doi: 10.1161/CIRCRESAHA.113.301565.

15. Jacquemet V, Henriquez CS. Genesis of complex fractionated atrial electrograms in zones of slow conduction: a computer model of microfibrosis. *Heart rhythm* (2009) 6(6):803-10. doi: 10.1016/j.hrthm.2009.02.026.

16. Balaban G, Halliday BP, Mendonca Costa C, Bai W, Porter B, Rinaldi CA, et al. Fibrosis Microstructure Modulates Reentry in Non-ischemic Dilated Cardiomyopathy: Insights From Imaged Guided 2D Computational Modeling. *Front Physiol* (2018) 9:1832. Epub 2019/01/09. doi: 10.3389/fphys.2018.01832.

17. Blanchard SM, Smith WM, Buhrman WC, Ideker RE, Lowe JE, editors. Computed bipolar electrograms from unipolar epicardial recordings. *Proc Comp Cardiol* 1988; 25-28.

18. Mukherjee RK, Costa CM, Neji R, Harrison JL, Sim I, Williams SE, et al. Evaluation of a real-time magnetic resonance imaging-guided electrophysiology system for structural and electrophysiological ventricular tachycardia substrate assessment. *Europace* (2019) 21(9):1432-41. Epub 2019/06/21. doi: 10.1093/europace/euz165.

In review

6. Figure Legends

Figure 1. Computational model setup. A sheet of myocardium (pink) is covered by a thin layer of bath (blue). The tissue was paced at the middle left edge (black triangle). Bipolar electrograms were measured at the centre of the tissue by subtracting the signals from electrodes (E) 1 and 2 – 1 mm apart (edge-to-edge).

Figure 2. Calculation of electrogram area in a bipolar electrogram recording. A) A representative bipolar electrogram recording. Signals above and below a noise threshold of +/- 0.05mV are shaded in red. b) Graph showing the cumulative sum of shaded area, where the peak value is the total electrogram area. Normalised electrogram area is calculated by dividing the total area by the signal amplitude (maximum – minimum).

Figure 3. Impact of altering sodium channel conductance and intracellular conductivity on electrogram morphology in a model of a propagating mose ventricular action potential. a) Simulated bipolar electrograms with decreasing sodium channel conductance (gNa) and intracellular conductivity (σi). Red shading shows the calculated electrogram area. Data are shown for electrode diameters of 0.1 and 1mm. b-d) Data showing changing signal amplitude (b), absolute electrogram area (EA), c), and (d) normalised EA (norm_EA) as a % of gNa and σi (presented data for 0.1mm electrode diameter).

Figure 4. Influence of altered sodium channel conductance and intracellular conductivity on electrogram morphology and its relationship with local conduction delay. a) Data showing the impact of altering electrode diameter on the relationship between normalised electrogram area (norm_EA) and local tissue conduction delay with altered sodium channel conductance (gNa) / intracellular conductivity (σ_i) in a computational model of a propagating mouse ventricular action potential. Data are shown for 3 different electrode diameters. b) The same data for bipolar electrogram amplitude.

Figure 5. Influence of electrode orientation on bipolar electrogram morphology in a model of a propagating mouse action potential. Data showing the impact of altering the orientation of the recording electrodes relative to the direction of propagation of the activation wavefront (electrode-wavefront angle) on bipolar electrogram morphology. a) Representative diagram showing change in electrode-wavefront angle. b&c) Data showing the change in bipolar electrogram amplitude and normalised electrogram area (norm_EA) as a function of the electrode-wavefront angle. 0^o represents the initial model conditions. Data are shown for

In review

varying levels of intracellular conductivity (σ_i). d&e) The same data plotted as a function of the local conduction delay between the recording electrodes.

Figure 6. Influence of simulated fibrosis on bipolar electrogram morphology in a model of a propagating mouse action potential (maps). Maps showing the impact of simulated regional fibrosis on the pattern of electrical activation (as analysed from a grid of unipolar electrograms), bipolar electrogram amplitude and normalised electrogram area (norm_EA).

Figure 7. Influence of simulated fibrosis on bipolar electrogram morphology in a model of a propagating mouse action potential (analysis). Quantitative analysis of the relationship between conduction delay and electrogram morphology in conditions of varying levels of tissue fibrosis (electrogram recorded within fibrotic tissue). a) Bipolar electrogram amplitude, b) normalised electrogram area (norm_EA).

Figure 8. Effects of sodium channel blockade and gap junction inhibition on electrogram morphology in isolated mouse hearts. a-c) Data showing the effects of increasing concentrations of flecainide on bipolar electrogram amplitude, absolute electrogram area (EA) and normalised EA (norm_EA). d-f) The same panels but for increasing concentrations of carbenoxolone. g&h) Correlation between norm_EA and local activation delay (as assessed from the difference in activation time between adjacent electrodes/unipolar electrograms). Difference from 0μmol/L; *p<0.05, **p<0.01, ***p<0.001. Data are mean ± SEM. Actual replicates are shown in grey. n=6-7 hearts per group.

Figure 9. Effects of low-flow ischaemia on electrogram morphology in isolated mouse hearts. Changes in electrogram morphology during low-flow global ischaemia in perfused mouse hearts. a) Representative bipolar electrogram recordings showing the change in electrogram morphology during a 120-second period of low-flow ischaemia and subsequent tissue reperfusion in a single mouse heart. The red shading indicates the calculated electrogram area. b-d) Mean data from 7 mouse hearts showing the changes in bipolar electrogram amplitude (b), absolute electrogram area (EA) (c), and amplitude-normalised EA (norm_EA) (d) in response to ischaemia-reperfusion. Different from 0; *p<0.05, **p<0.01, ***p<0.001. Data are mean ± SEM. Actual replicates are shown in grey. n=7 hearts.

Figure 10. Stability of bipolar electrogram metrics in isolated mouse hearts. Data showing the stability of measures of electrogram morphology in isolated mouse hearts. EA = electrogram area. norm_EA=amplitude-normalised electrogram area. n=6 hearts.

In review

Figure 11. Influence of flecainide on electrogram morphology in perfused guinea pig hearts. a) Mean data from 6 experiments showing the effects of switching to buffer containing 4μmol/L flecainide on bipolar electrogram amplitude and amplitude-normalised electrogram area (norm_EA). Different from time 0; *p<0.05, **p<0.01, ***p<0.001. Data are mean ± SEM. Actual replicates are shown in grey. n=6 hearts.

In review

Figure 1.JPEG

In review

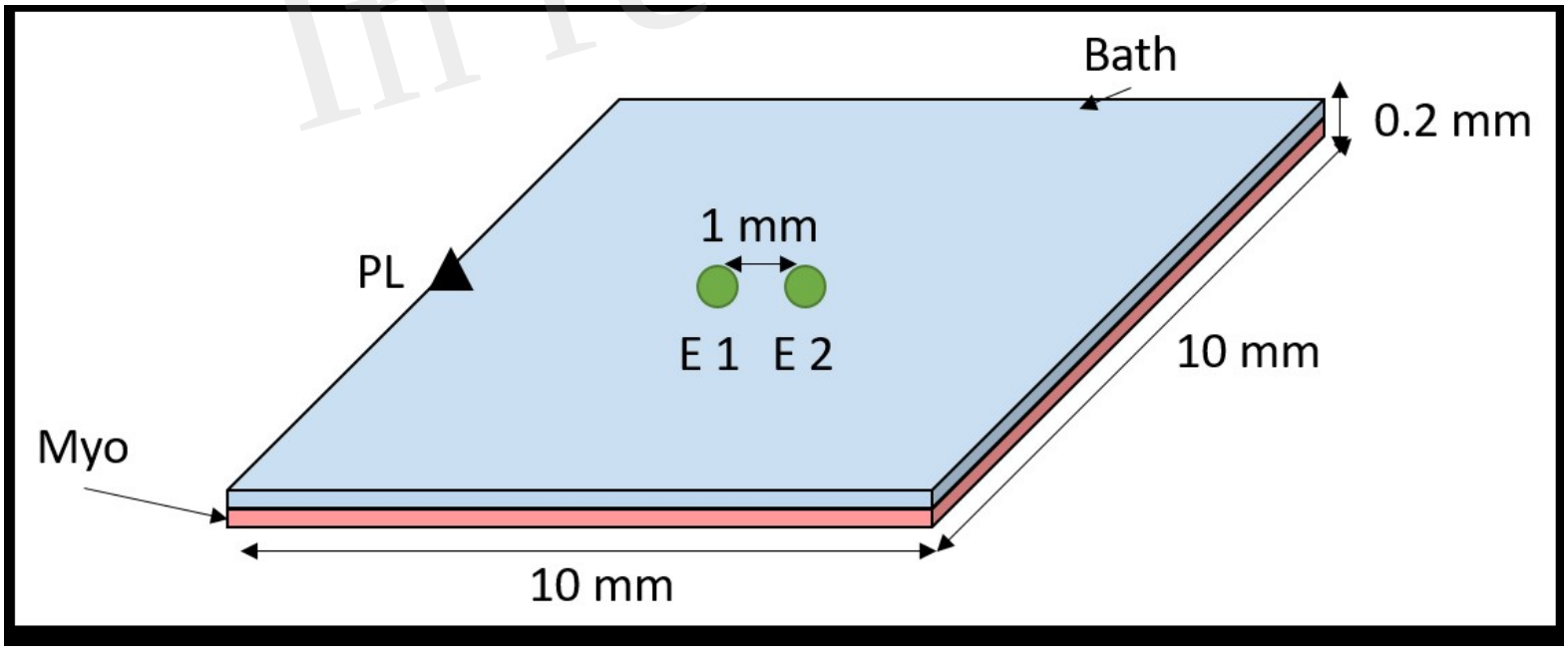

Figure 2.JPEG

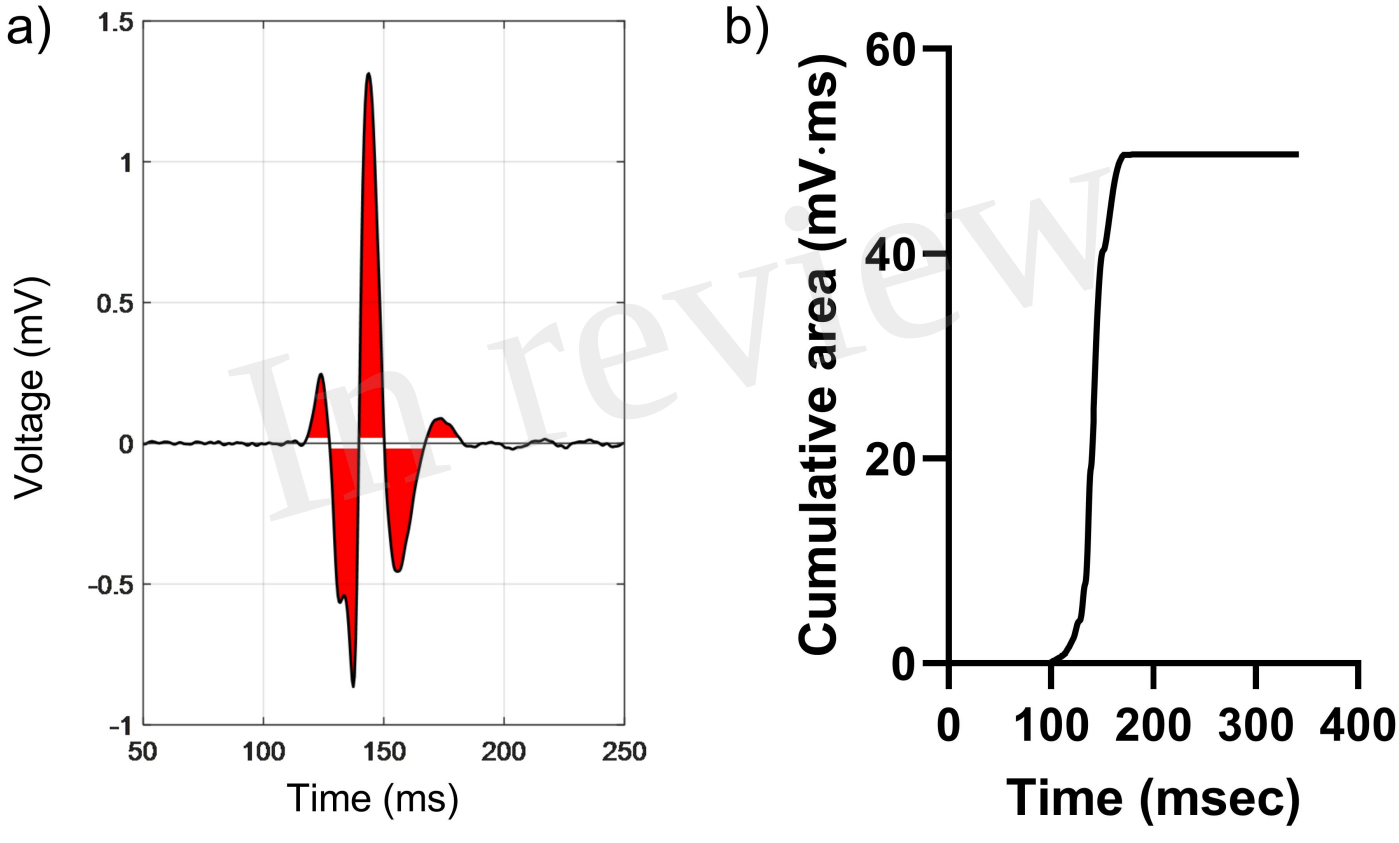

In review

Figure 3.JPEG

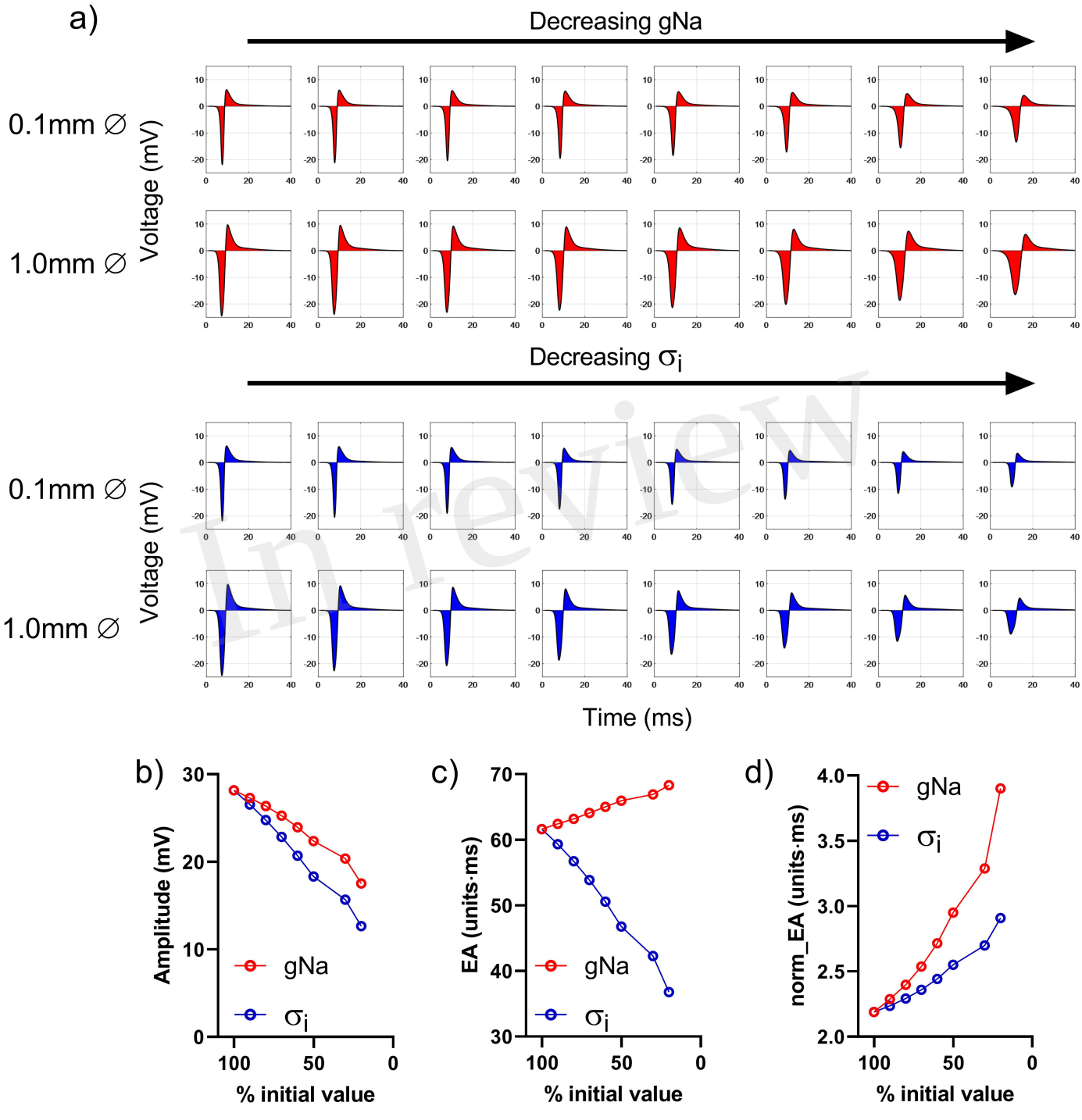

In review

Figure 4.JPEG

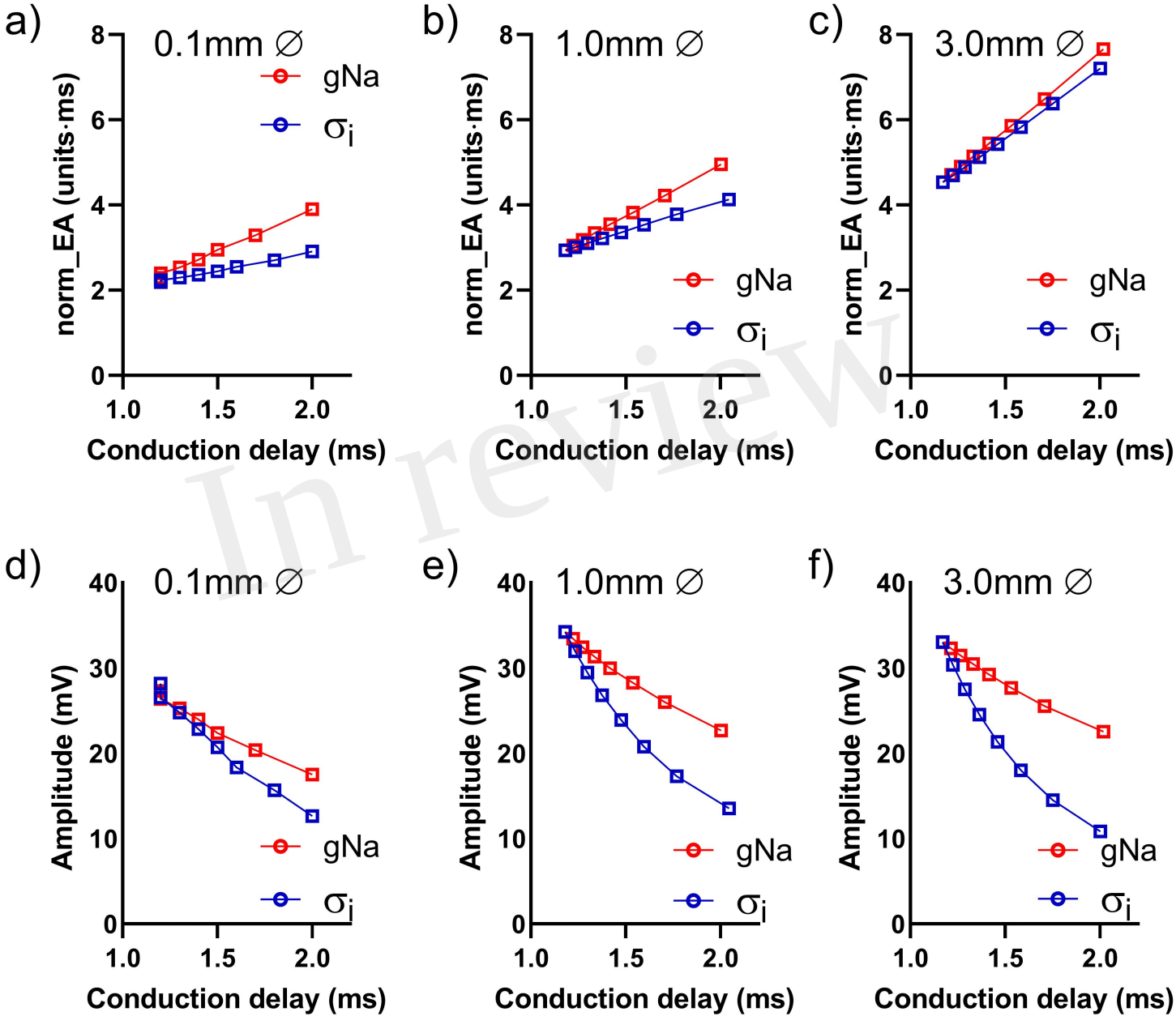

In review

Figure 5.JPEG

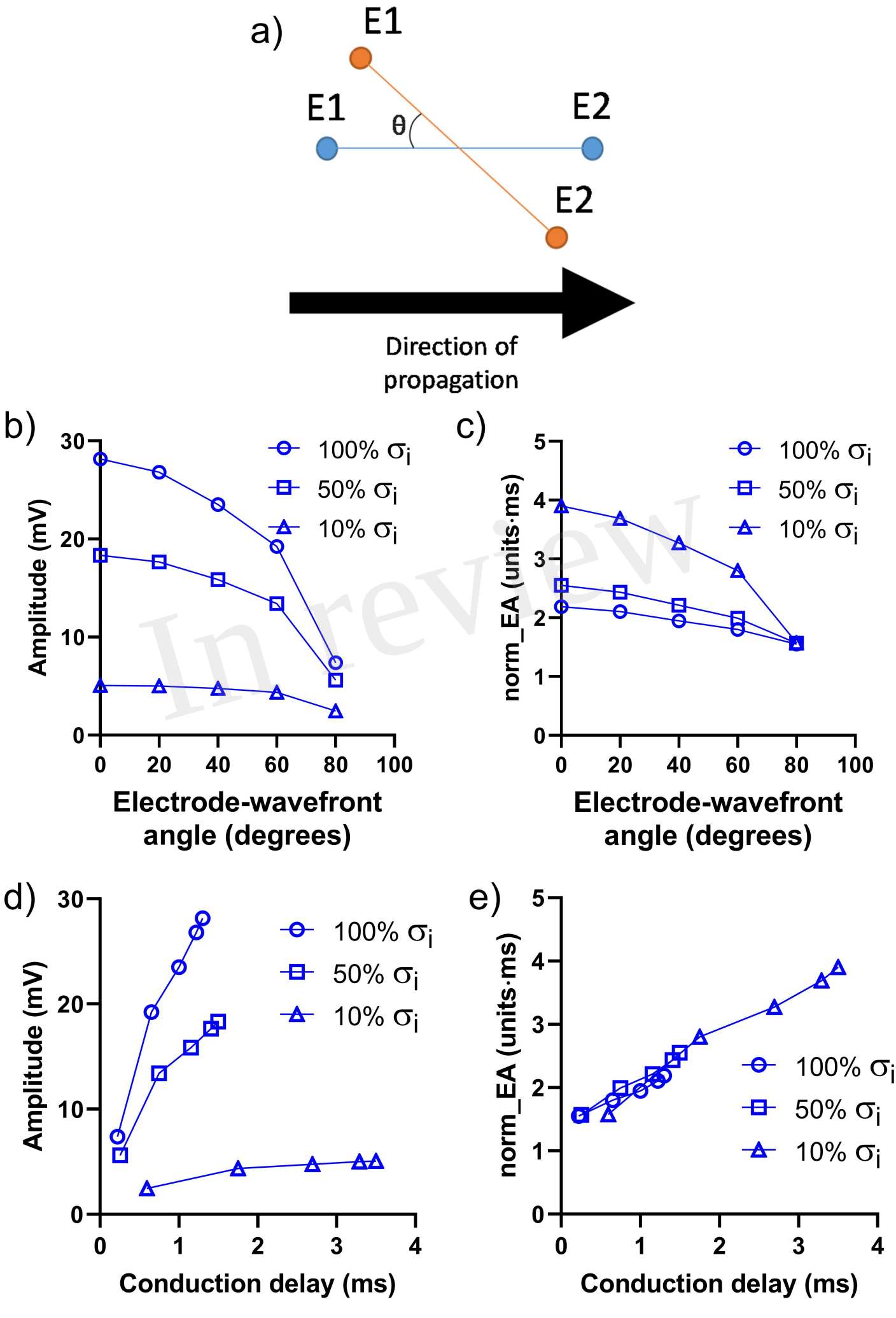

In review

Figure 6.JPEG

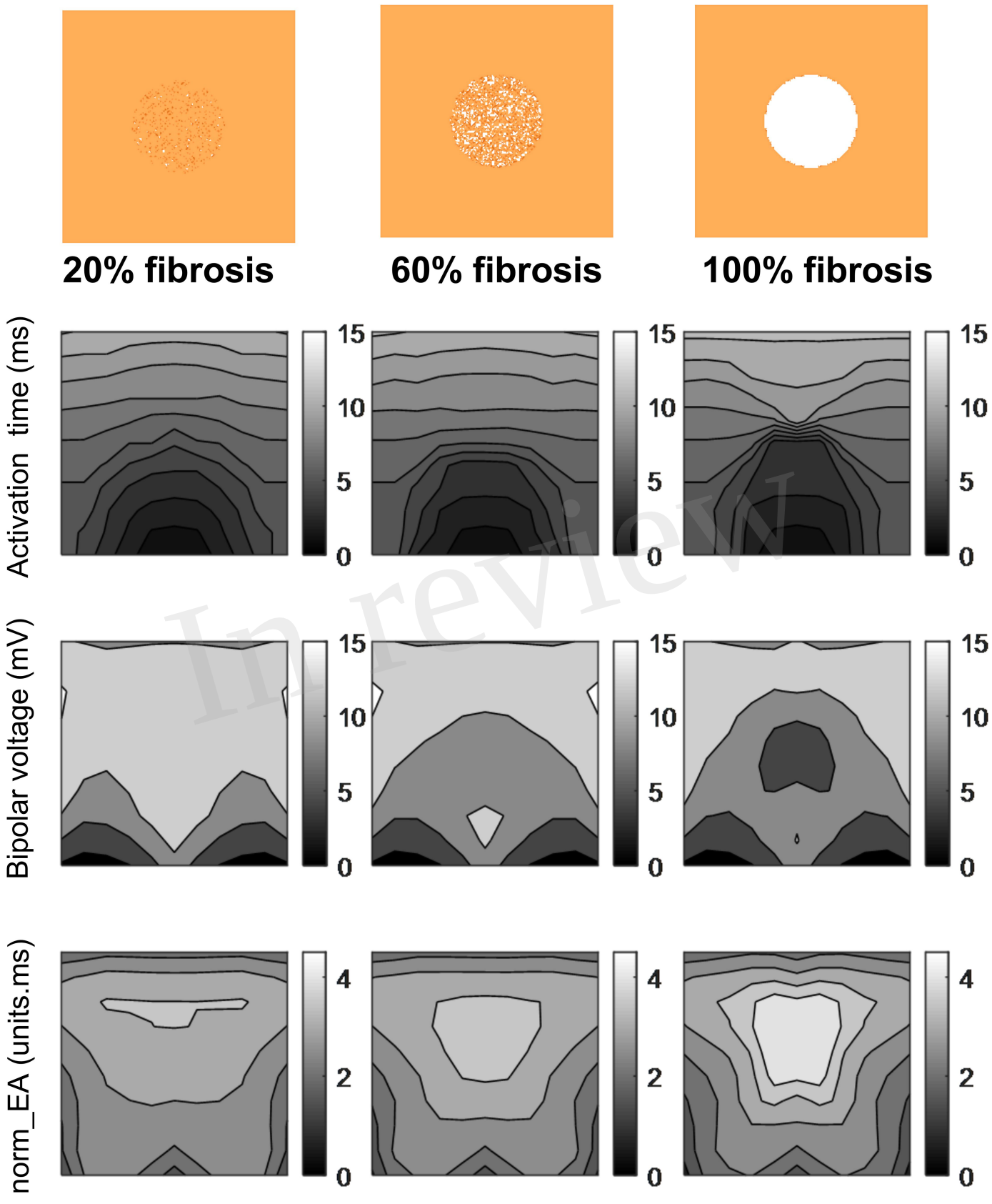

In review

Figure 7.JPEG

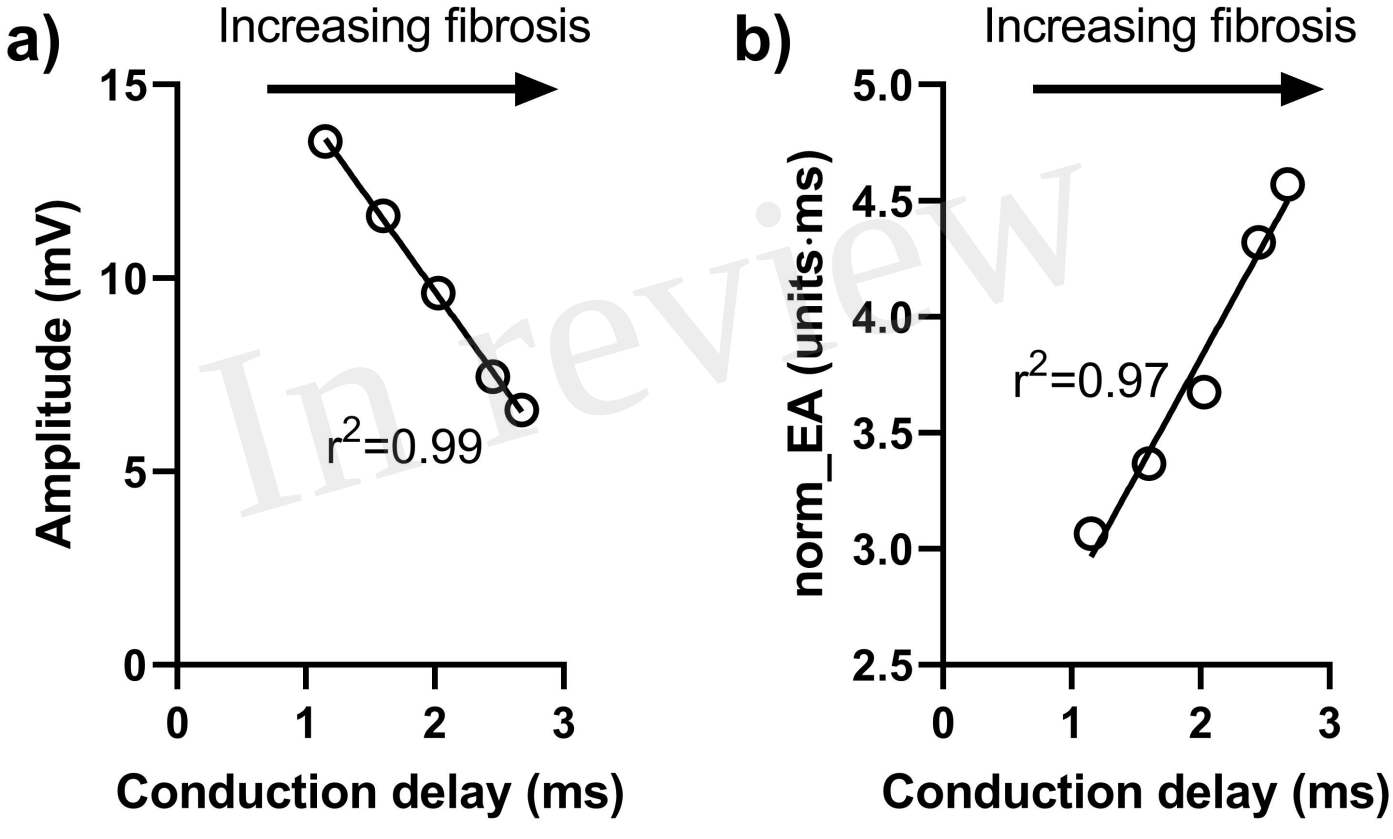

In review

Figure 8.JPEG

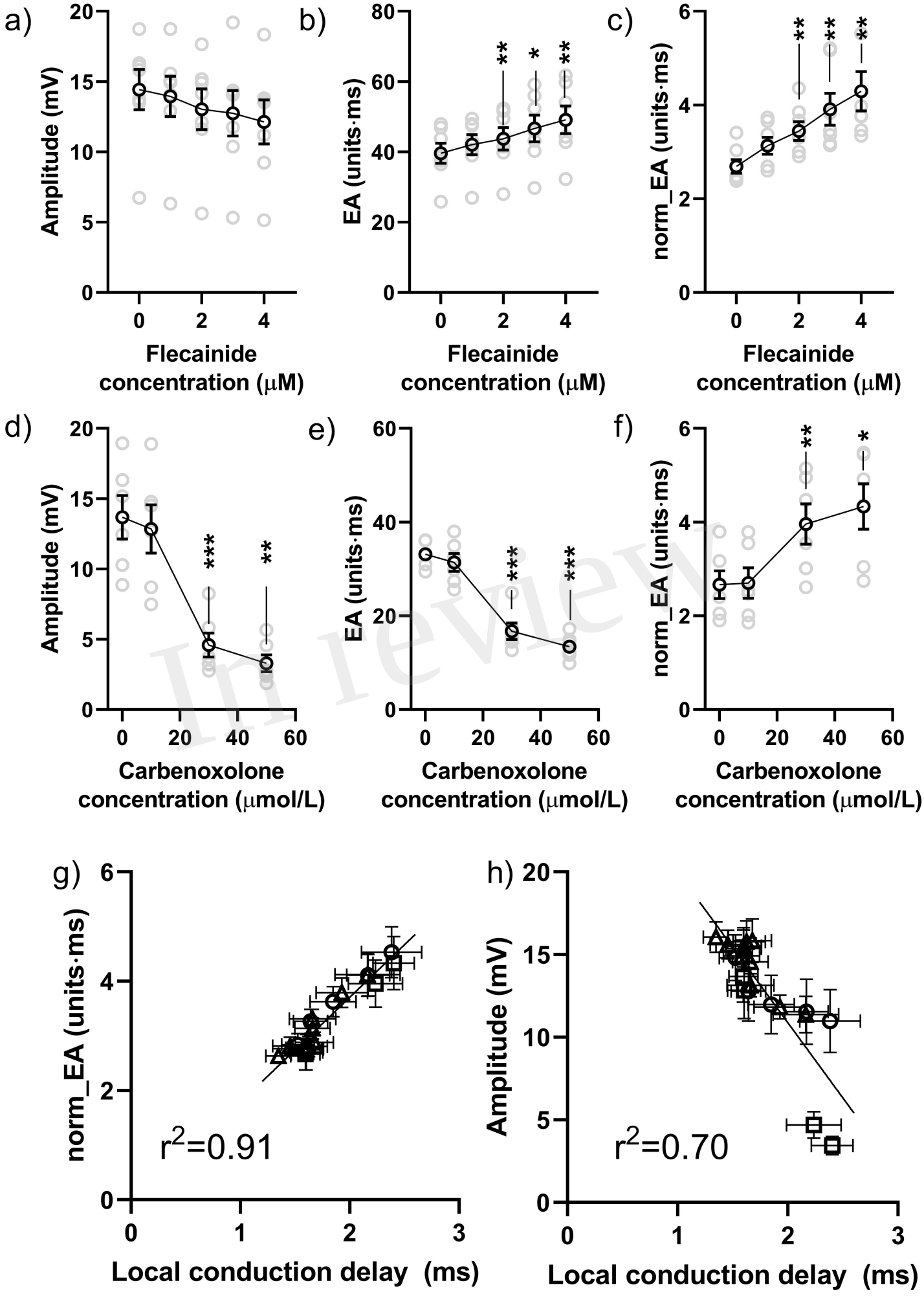

In review

Figure 9.JPEG

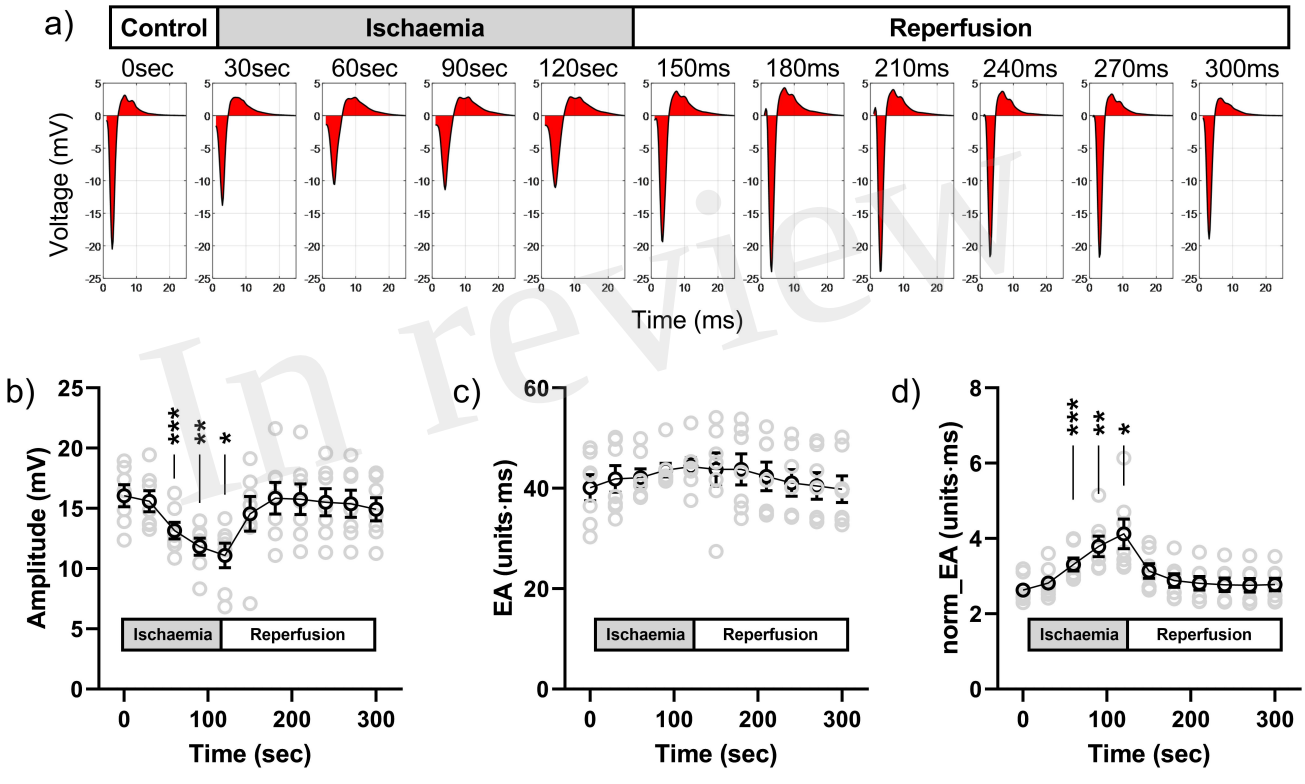

In review

Figure 10.JPEG

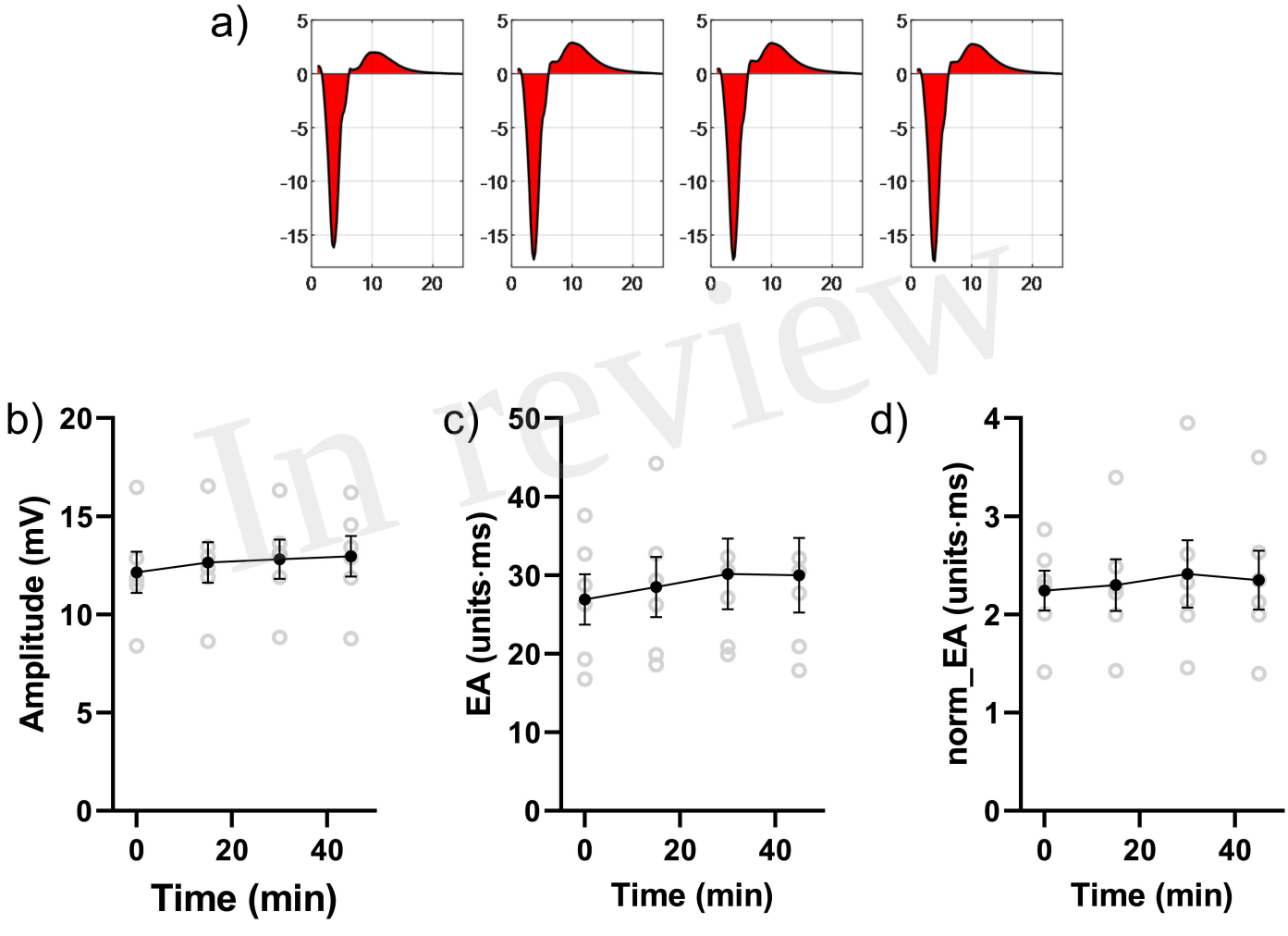

In review

Figure 11.JPEG